Study of the carbon material electrolyte interface

R. Yazami [a,*], M. Deschamps [a], S. Genies [a], J.C. Frison [b]

[a] *LEPMI, ENSEEG, BP 75, 38402 St Martin d'Hères, France*
[b] *CNET-Centre Lannion B, 2 route de Trégastel, 22301 Lannion Cedex, France*

Abstract

The formation mechanism of the passivation film on the surface of carbon-based electrodes during the first electroreduction was studied by chronopotentiometry and impedance spectroscopy. Two types of electrolytes are compared: ethylene carbonate-based liquid and poly(ethylene oxide)-based solid state electrolytes. The differences in stability towards reduction and in mobility of the solvent molecules in these electrolytes suggest two different mechanisms of reduction: (i) decomposition of the solvent in the liquid electrolyte system, and (ii) formation of an immobilized dense layer in the solid electrolyte system. The chemical diffusion coefficient was also determined by impedance spectroscopy at increased amounts of lithium in the carbon electrode. The film formation and the diffusion are correlated. © 1997 Elsevier Science S.A.

1. Introduction

Carbon-based negative electrodes undergo a surface passivation at the interface with the electrolyte either in liquid or in solid states during their first electroreduction (charge of the lithium-ion battery) [1,2]. In such a reaction, part of the active lithium is consumed during the reduction of the electrolyte (solvent/lithium salt) and cannot be restored within the working voltage range of the carbon electrode. This lost lithium accounts for the loss of capacity of the cell and constitutes the main component of the faraday yield γ_F which is the ratio of the amount of lithium recovered to that transferred to the electrode during the first cycle. However, the passivation plays an important role in the cycleability of the negative electrode and as consequence of that of lithium-ion battery. It prevents lithium from being intercalated in the solvated state which would lead to the exfoliation (swelling) of the carbon. In a mechanism which is not clear yet, solvated lithium in the liquid electrolyte looses its solvatation shell during its migration into the passivation film and penetrates the carbon host structure in the 'dry' form. In addition, the passivation film also prevents the electrolyte from further reduction by the active lithium and thus limiting the degradation of the electrolyte.

In this work, we carried out a comparative study of the interface properties between carbon negative electrode and a liquid or solid-state electrolyte. Even though the mechanism of passivation has not been fully clarified, differences in the evolution of the interfacial properties in liquid and solid electrolyte suggested a different mechanism of 'film' formation. Also a tentative correlation between the passivation and lithium chemical diffusion in graphitic carbon will be presented and discussed.

2. Experimental

For liquid electrolyte-based cells, the electrode was prepared as follows: a mixture of 80 wt.% of natural graphite (average grain size 4 μm), 10 wt.% of poly(vinilydene difluoride)-copolymer (12% of hexafluoropropylene) and 10 wt.% of carbon black, was stirred mechanically, then acetone was added for a better homogeneization. The mixture was ball-milled for 60 min, then dried in air, and pressed to form a pellet of 13 mm in diameter and ~0.3 mm in thickness. It was dried under vacuum at 80 °C for 10 h. 1 M electrolyte solutions of $LiPF_6$, $LiBF_4$, $LiClO_4$ were prepared in dry box filled with argon (less than 1 ppm of $H_2O + O_2$) using the same solvent mixture of volumic composition ethylene carbonate:propylene carbonate:dimethoxyethane (1:1:2).

For polymer electrolyte-based cells, the mixture consisted of 60 wt.% of carbon (coal pitch coke, HTT 1000 °C), 30 wt.% of polyethylene oxide, 7 wt.% of acetylene black and 3 wt.% of lithium salt. After ball-milling in the presence of

* Corresponding author.

acetonitrile for 1 h, the liquid slurry was spread onto a stainless-steel disc of 16 mm in diameter, and then dried in air, and in vacuum at 60 °C for 10 h.

Test cells consisted of coin-type 2430 (24 mm diameter, 3 mm thickness) having metallic lithium disc of 20 mm in diameter as the negative pole, microporous polyethylene separator (Celgard 2400) in the liquid electrolyte ones or $P(EO)_8LiX$ film as the separating electrolyte in the solid electrolyte cases. In the latter the $P(EO)_8LiX$ film was mechanically pressed onto the carbon-based electrode at 80 °C to improve their contact efficiency before sealing the cell.

Cells were operated at 25 ± 0.2 °C for the liquid electrolyte and at 100 ± 1 °C for the polymer electrolyte. $C/10$ constant current (37.2 mA/g of active carbon) was applied and the

Fig. 1. Potentials of the first galvanostatic discharge where are taken an impedance spectra.

discharge was potential limited. When the potential limit was reached, the cell was allowed to rest for several hours until the potential drive was <0.1 mV/min, and then complex impedance measurement was performed. The frequency range was 0.01 Hz–100 kHz and the voltage amplitude was 10 mV. The lithium chemical diffusion coefficient was determined following methods described by Cabanel et al. [3] or Ho et al. [4].

3. Results and discussion

3.1. Liquid electrolyte

Fig. 1 shows a typical first discharge curve obtained with a fine powder (4 μm) of natural graphite as the active material of the carbon electrode. It shows the three voltage positions where a.c. impedance spectra were taken: initial open-circuit voltage, 800 and 5 mV versus Li/Li^+.

Fig. 2 gives the corresponding Nyquist diagrams obtained with different lithium salts: (a) $LiClO_4$ (OCV = 1.94 V); (b) $LiBF_4$ (OCV = 2.64 V); (c) $LiCF_3SO_3$ (OCV = 1.80 V); (d) $LiN(CF_3SO_2)_2$ (OCV = 1.34 V), and (e) $LiPF_6$ (OCV = 2.66 V). The numbers given in arabic character refer to the frequency of the a.c. signal as powers of 10 (i.e. $3 \rightarrow 10^3$ Hz).

While the spectra taken at the initial state show two semicircles and a Warburg curve in all five electrolytes (curve I), an important change in curve shapes is observed in the cases of $LiClO_4$ and $LiBF_4$ when cells were discharged to 0.8 V (curve II) in comparison with the other salts. These curves

Fig. 2. Impedance spectra obtained at different electrode potentials during the first discharge with different lithium salts.

Table 1

Lithium chemical diffusion coefficient, D_{Li}, obtained with different lithium salts

Lithium salts	D_{Li} ($\times 10^{-7}$ cm^2 s^{-1})
LiBF$_4$	2.28
LiCF$_3$SO$_3$	3.42
LiN(CF$_3$SO$_2$)$_2$	2.64
LiPF$_6$	2.24

Fig. 3. Composition dependence of the charge transfer (CT), persistion film (Films) and electrolyte impedance in Li/POE–LiClO$_4$/Li$_x$C$_6$ (from coke) during the first carbon reduction.

II show a monotonous increase of the imaginary part versus the real one, with no maximum even at lower frequencies. This may result from either lithium diffusion in a highly heterogeneous film or from any phenomena that tends to hinder the diffusion of charged species to the electrode/electrolyte interface. This would be the case if a gaseous layer is formed on the carbon surface as a result of the electrolyte reduction. In LiClO$_4$ and LiBF$_4$, the anion seems to play an important role in the activation of such gas formation. A striking behavior is observed with LiCF$_3$SO$_3$ where the impedance associated with the charge transfer decreases at 0.8 V, and then re-increases at the final fully lithiated state of graphite. The decomposition product of CF$_3$SO$_3^-$ seems to have a catalytic effect on the electrode reaction.

LiN(CF$_3$SO$_2$)$_2$ and LiPF$_6$ have the most stable spectra as a function of the lithiation state of the graphite electrode. The decomposition products of their respective anions seem to form a uniform and stable thin layer which properties do not significantly evolve with the lithium amount. No electrode shielding (i.e. gassing) was observed at intermediary potential as in case of ClO$_4^-$ and BF$_4^-$. The effect of the nature of the anion of the lithium salt on the mechanism of the carbon passivation deserves a specific study which is out of the purpose of this work.

Another interesting effect concerns the lithium chemical diffusion coefficient D_{Li} which was determined after the first discharge/charge cycle at the end of charge ($x = 0$ in Li$_x$C$_6$) in order to eliminate the effect of the film formation. Table 1 gives the value of D_{Li} obtained with different lithium salts. Though the order of magnitude is the same, the highest value was reached with LiN(CF$_3$SO$_2$)$_2$ and the lowest was with LiPF$_6$ and LiBF$_4$ ($\cong 2.28 \times 10^{-7}$ cm^2 s^{-1}). The anion effect on the lithium diffusion seems to be milder than on the passivation. The coulomb interaction between Li$^+$ and the anions at the carbon layer edges might account for this difference. This interaction seems to be stronger in quasi spherical anions (BF$_4^-$ and PF$_6^-$) than in more elongated ones (N(CF$_3$SO$_2$)$_2^-$ and CF$_3$SO$_3^-$).

3.2. Polymer electrolyte

In this section we show a typical evolution of the interfacial properties between carbon and polyethylene oxide during the first discharge of the Li/PEO–LiClO$_4$)/coke cell at 100 °C.
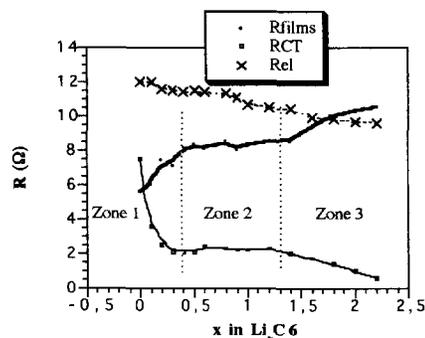
The Cole–Cole plot can be generally fitted with two semi-circles and a Warburg branch [2]. An equivalent electric circuit may consist of a series of charge transfer (CT), passivation film (Films) and diffusion impedance. Each of them can be plotted as a function of the amount of lithium transferred to the electrode. Fig. 3 shows such a evolution for the CT and Films resistance (real part, R_{CT} and R_{Films}). R_{CT} decreases, stabilizes, and then decreases again with the electrode reaction rate while concomitantly R_{Films} increases then stabilizes. The decrease of R_{CT} during the first phase ($0 < x < 0.4$) at a potential at which lithium is not yet intercalated was ascribed to the enhancement of the surface contact between the carbon and the polymer electrolyte via lithium bridges [2]. As a matter of fact, the lithium consumed during this phase is highly irreversible which implies that the electron transferred during the reduction might be back donated to the electrolyte. Since PEO is known to be very stable versus reduction, we suggested that the electron is captured by the empty external molecular orbital of the oxygen of the ether group. This should lead to the formation of C–Li$^+$–O$^-$–(CH$_2$)$_2$ bonding at the carbon surface. PEO tends to cover more efficiently the external surface of the active carbon, therefore the energy gap necessary to transfer Li$^+$ from the electrolyte will decrease. Such mechanism was described by as the 'Zipper Model' [2]. The lithium involved in the C–Li$^+$–O$^-$–(CH$_2$)$_2$ bonding is strongly attached to the carbon and consequently cannot be easily re-oxidized when the current is reversed. Such a 'binding' lithium accounts for the low Faraday yield of the first cycle in polymer-based lithium-ion batteries. In more disordered carbons, the initial evolution of R_{CT} versus x is much more complicated than in the case of coke. However, there is a clear relationship between the amount of the irreversible lithium and the size of the carbon crystallites. In 'nanometric disordered carbons' (semi-cokes), such an amount can be higher than 1000 mAh/g [5]. Fig. 3 shows also the composition dependence of the electrolyte resistance (R_{el}) which slightly decreases probably as the thickness of the space available for the electrolyte decreases at the expense of that of the film.

References

[1] R. Fong, U. van Sacken and J.R. Dahn, *J. Electrochem. Soc., 137* (1990) 2009; J.O. Besenhard, M. Winter, J. Yang and W. Biberacher, *J. Power Sources, 54* (1995) 228.

[2] R. Yazami and M. Deschamps, *Mater. Res. Soc. Symp. Proc., 369* (1995) 165.

[3] R. Cabanel, G. Barral, J.P. Diard, B. Legorrec and C. Montella, *J. Appl. Electrochem., 23* (1993) 93.

[4] C. Ho, I.D. Raistrick and R.A. Huggins, *J. Electrochem. Soc., 127* (1980) 343.

[5] R. Yazami and M. Deschamps, *J. Power Sources*, (paper N° I-A-17).